

 Open access • Journal Article • DOI:10.1063/1.4927057

## Multi-quartz-enhanced photoacoustic spectroscopy — Source link

Yufei Ma, Xin Yu, Guang Yu, Xudong Li ...+4 more authors

**Institutions:** Harbin Institute of Technology, Rice University

**Published on:** 15 Jul 2015 - Applied Physics Letters (AIP Publishing LLC)

**Topics:** Photoacoustic effect and Photoacoustic spectroscopy

Related papers:

- [Quartz-enhanced photoacoustic spectroscopy](#)
- [Off-beam quartz-enhanced photoacoustic spectroscopy.](#)
- [QEPAS based ppb-level detection of CO and N2O using a high power CW DFB-QCL](#)
- [Intracavity quartz-enhanced photoacoustic sensor](#)
- [Short-lived species detection of nitrous acid by external-cavity quantum cascade laser based quartz-enhanced photoacoustic absorption spectroscopy](#)

Share this paper:    

View more about this paper here: <https://typeset.io/papers/multi-quartz-enhanced-photoacoustic-spectroscopy-4m47hx179r>

## Multi-quartz-enhanced photoacoustic spectroscopy

Yufei Ma,<sup>1,2,a)</sup> Xin Yu,<sup>1</sup> Guang Yu,<sup>1</sup> Xudong Li,<sup>1</sup> Jingbo Zhang,<sup>1</sup> Deying Chen,<sup>1</sup> Rui Sun,<sup>2</sup> and Frank K. Tittel<sup>3</sup>

<sup>1</sup>National Key Laboratory of Science and Technology on Tunable Laser, Harbin Institute of Technology, Harbin 150001, China

<sup>2</sup>Post-doctoral Mobile Station of Power Engineering and Engineering Thermophysics, Harbin Institute of Technology, Harbin 150001, China

<sup>3</sup>Department of Electrical and Computer Engineering, Rice University, 6100 Main Street, Houston, Texas 77005, USA

(Received 29 April 2015; accepted 8 July 2015; published online 15 July 2015)

A multi-quartz-enhanced photoacoustic spectroscopy (M-QEPAS) sensor system for trace gas detection is reported. Instead of a single quartz tuning fork (QTF) as used in QEPAS technique, a dual QTF sensor platform was adopted in M-QEPAS to increase the signal strength by the addition of the detected QEPAS signals. Water vapor was selected as the target analyte. M-QEPAS realized a 1.7 times signal enhancement as compared to the QEPAS method for the same operating conditions. A minimum detection limit of 23.9 ppmv was achieved for the M-QEPAS sensor, with a calculated normalized noise equivalent absorption coefficient of  $5.95 \times 10^{-8} \text{ cm}^{-1} \text{ W}/\sqrt{\text{Hz}}$ . The M-QEPAS sensor performance can be further improved when more QTFs are employed or an acoustic micro-resonator architecture is used. © 2015 AIP Publishing LLC.

[<http://dx.doi.org/10.1063/1.4927057>]

Trace gas detection based on laser absorption spectroscopy is a topic of considerable interest in recent years because of its many important applications in atmospheric chemistry<sup>1</sup> and combustion diagnosis.<sup>2</sup> Sensing methods based upon laser power buildup sensing methods have the merits of high sensitivity and selectivity. Among these methods, photoacoustic spectroscopy (PAS) is one of the most effective trace gas detection technologies. PAS employs a broadband microphone for acoustic wave detection and is characterized by a low cost and robust architecture. However, most microphone-based PAS cells have a low resonance frequency, which makes cells more sensitive to environmental and sample gas flow noise. Moreover, the size of the typical photoacoustic cell is relatively large.<sup>3</sup>

A recent improvement of microphone-based PAS is the quartz-enhanced photoacoustic spectroscopy (QEPAS) technique.<sup>4</sup> This technique uses a low cost and commercially available millimeter sized piezoelectric quartz tuning fork (QTF) as an acoustic wave transducer, which possesses a high selectivity and immunity to ambient acoustic noise. In QEPAS technology, instead of a large photoacoustic cell as in conventional PAS, the acoustic energy is accumulated in the sharply resonant QTF. Therefore, a limitation of the gas cell size does no longer exist and the cell volume can be reduced, and even the cell can be optional. QEPAS has been successfully applied to trace gases detection,<sup>5,6</sup> and different sensor architectures due to the advantages of high sensitivity, selectivity, and compactness were developed such as an off-beam QEPAS sensor,<sup>7</sup> an intracavity QEPAS sensor,<sup>8</sup> and an evanescent-wave QEPAS sensor.<sup>9</sup>

Up to now, all the QEPAS sensors use one QTF to detect acoustic wave signal generated by laser absorption. In this paper, we report on the development of a gas sensing

technique based on a multiple QTFs detection scheme, which we termed multi-quartz-enhanced photoacoustic spectroscopy (M-QEPAS). In M-QEPAS technology, the acoustic wave signal will be detected by multiple QTFs simultaneously, and the electrical signals generated by QTFs will be added in order to increase the effective signal amplitude. In this paper, the number of QTFs was selected to be two to demonstrate the M-QEPAS technology, and water vapor (H<sub>2</sub>O) was chosen as the target analyte.

Commercially available QTFs with a resonant frequency  $f_0$  of  $\sim 32.76$  kHz is usually used in QEPAS sensors. The diameter of the QTF enclosure is  $\sim 3$  mm, and the gap between two prongs is  $\sim 300$   $\mu\text{m}$ . The focused laser should pass through the gap without touching, otherwise the QTF noise level will increase. In this paper, two QTFs with  $f_0$  of 32.76 kHz were used and mounted parallel pointing in opposite directions for a convenient spatial arrangement, as shown in Fig. 1. A 1.395  $\mu\text{m}$  continuous wave, distributed feedback (CW-DFB) fiber-coupled diode laser with a spectral linewidth of 10 MHz was employed as the laser excitation source. The laser beam quality was measured by a 90/10 traveling knife-edge method, and the beam quality factor  $M^2$  was found to be 1.03 at an output power of 12.6 mW, when the 7168.4  $\text{cm}^{-1}$  H<sub>2</sub>O absorption line was targeted. The beam was collimated using a fiber collimator with a focal length of 18.67 mm. Subsequently, the laser beam was focused between the QTFs prongs inside an acoustic detection module (ADM) using a 60 mm focal length plano-convex CaF<sub>2</sub> lens. This optical scheme resulted in a spatial range of 9 mm, and in this range the laser beam diameter was  $< 300$   $\mu\text{m}$ , which can be used for placing the two QTFs conveniently.

The experimental sensor system is shown in Fig. 2. After passing through ADM, the laser beam was monitored by an optical power meter for alignment verification of the

<sup>a)</sup>Electronic mail: mayufei926@163.com

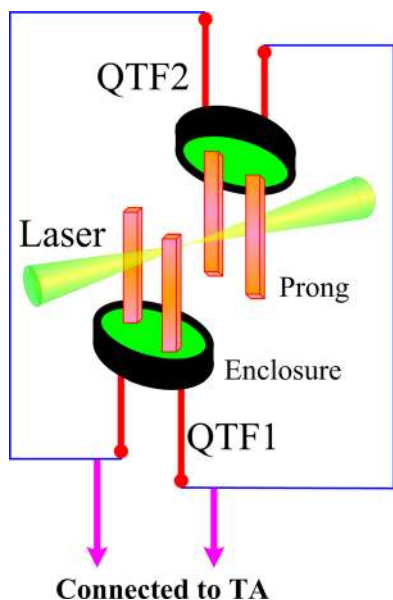


FIG. 1. Schematic of M-QEPAS with two QTFs.

sensor system. Modulation of the laser current was implemented by applying a sinusoidal dither to the direct current ramp of the diode laser at half of the QTF resonance frequency ( $f=f_0/2$ ). The piezoelectric signal generated by the QTF was detected by a low noise transimpedance amplifier with a  $10\text{ M}\Omega$  feedback resistor and converted into a voltage. Subsequently, this voltage was transferred to a custom built control electronics unit (CEU). The CEU provides the following three functions: (1) measurement of the QTF parameters, i.e., the quality factor  $Q$  and resonant frequency  $f_0$ ; (2) modulation of the laser current at the frequency  $f=f_0/2$ ; and (3) measurement of the  $2f$  component generated by the QTF.

Air present in a closed laboratory environment was employed as the target analyte, which contained  $0.21\%$   $\text{H}_2\text{O}$  as determined by means of a direct absorption method. The fluctuation of water vapor concentration was  $<5\%$ . The operating pressure was  $1\text{ atm}$ , and the measured parameters of the resonant frequency,  $Q$  factor, phase, and detection bandwidth for different QTFs are listed in Table I. A performance comparison of the M-QEPAS sensor and a QEPAS sensor with QTF1 and QTF2, respectively, was carried out. The integration time for QEPAS and M-QEPAS sensors system was  $1\text{ s}$  and the detection bandwidth for the two sensors was the same. The distance between QTF1 and QTF2 was

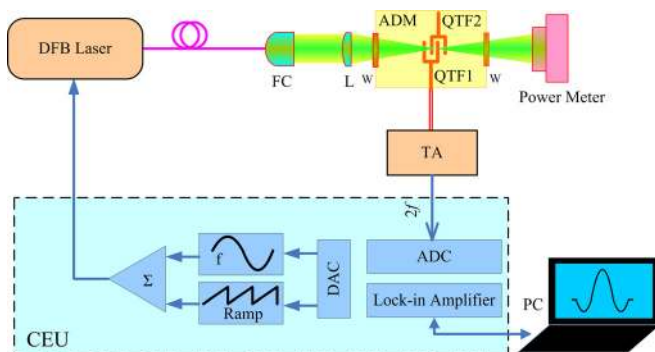
FIG. 2. Schematic of M-QEPAS sensor system. FC: fiber collimator; L: plano-convex lens; W:  $\text{CaF}_2$  window; and TA: transimpedance amplifier.

TABLE I. Parameters for different QTFs at experimental condition.

QTF no.	Resonant frequency $f_0$ (Hz)	$Q$ factor	Phase (deg)	Detection bandwidth $\Delta f$ (Hz)
QTF1	32756.9	5939	-23	5.52
QTF2	32757.9	5898	-44	5.55
QTF1 + QTF2	32757.3	5327	See Fig. 4	6.15

$150\ \mu\text{m}$  in the M-QEPAS system. The experimental results, shown in Fig. 3, illustrate the influence of the laser modulation depth on the signal amplitude measured at the targeted  $7168.4\text{ cm}^{-1}$   $\text{H}_2\text{O}$  absorption line. With the same modulation depth, the QEPAS signal levels using QTF1 and QTF2, respectively, were almost the same, while the M-QEPAS signal level was larger. The M-QEPAS signal amplitude increased with the modulation depth, but when the modulation depth was  $>0.492\text{ cm}^{-1}$ , no further significant change was observed. At a modulation depth of  $0.492\text{ cm}^{-1}$ , the signal levels were  $0.77\text{ mV}$ ,  $0.76\text{ mV}$ , and  $1.08\text{ mV}$  for sensors employing QTF1, QTF2, and QTF1 + QTF2, respectively.

The M-QEPAS signal amplitude and phase as a function of distance between QTF1 and QTF2 are shown in Fig. 4. When the distance between QTF1 and QTF2 was zero, there was no signal. With increasing distance between QTF1 and QTF2, the M-QEPAS signal amplitude and phase increased, but when the distance was  $>600\ \mu\text{m}$ , the M-QEPAS signal amplitude was no longer impacted by the distance between the two QTFs. This observed behavior is due to the coupling of the acoustic wave fields between QTF1 and QTF2.

The measured  $2f$  QEPAS signal and noise at a modulation depth of  $0.492\text{ cm}^{-1}$  for QTF1, QTF2, and QTF1 + QTF2 is shown in Fig. 5, respectively. The distance between QTF1 and QTF2 in M-QEPAS was  $600\ \mu\text{m}$ , and the signal amplitude was  $1.32\text{ mV}$ . Compared with signal levels of  $0.77\text{ mV}$  and  $0.76\text{ mV}$  for sensors employing QTF1 and QTF2, respectively, M-QEPAS resulted in a  $\sim 1.7$  times signal enhancement. For optimal conditions, the signal enhancement of M-QEPAS (using two QTFs) should be two times compared to a single QTF. This inconsistency can be explained by the following fact. In order to obtain the

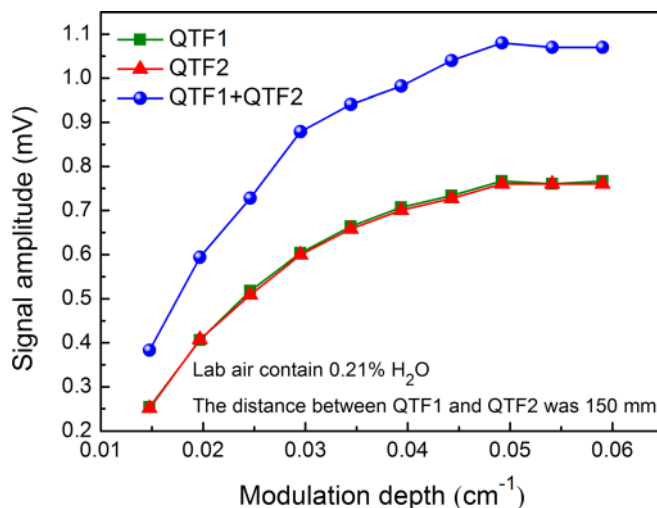


FIG. 3. Measured QEPAS signal amplitude as a function of laser modulation depth.

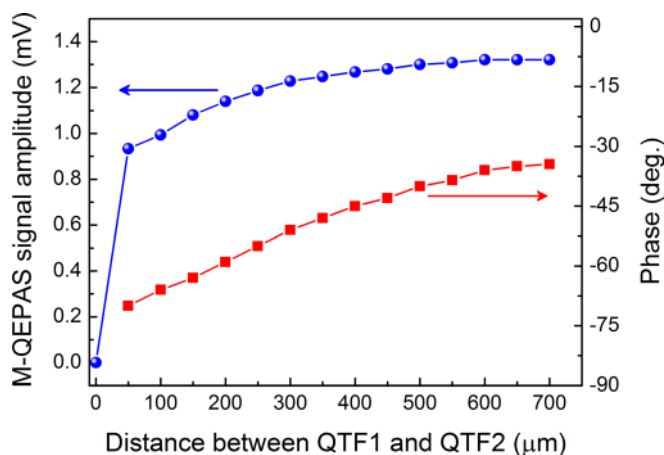


FIG. 4. M-QEPAS signal amplitude and phase at modulation depth of  $0.492\text{ cm}^{-1}$  as a function of distance between QTF1 and QTF2.

maximum signal strength, the modulation of the laser current should be at half of the QTF resonance frequency ( $f=f_0/2$ ). In M-QEPAS technology, the acoustic wave signal will be detected by multiple QTFs simultaneously, and the electric signal generated by QTFs will be added together. The measured resonance frequency  $f_0$  of QTF1+QTF2 was  $32757.3\text{ Hz}$ , and hence the modulation of the laser current was set to  $32757.3/2\text{ Hz}$ . However, the  $32757.3\text{ Hz}$  was not the same as that for QTF1 and QTF2 (see Table I). Therefore, QTF1 and QTF2 in M-QEPAS could not give the strongest response. Furthermore, there was a small difference in phase of QTF1 and QTF2. The smaller difference in resonant frequency and phase of QTFs will result in a greater signal improvement of M-QEPAS. It should be noted the parameters of resonant frequency and phase of QTF change with pressure. For M-QEPAS, when the experimental conditions are varied, if the difference in resonant frequency and phase between QTF1 and QTF2 is too large the signal enhancement decreases, it requires re-optimization of the QTFs. A better approach is to maintain the experimental conditions of the M-QEPAS sensor system using an in-line pressure controller.

The sensor noise was determined as a standard deviation from the signal far from the targeted absorption line. The  $1\sigma$  noise level was  $17\text{ }\mu\text{V}$ ,  $15\text{ }\mu\text{V}$ , and  $15\text{ }\mu\text{V}$  for QTF1, QTF2, and QTF1+QTF2, respectively. There is no obvious difference in noise levels when using a single QTF and multiple QTFs. A minimum detection limit (MDL) of  $46.4\text{ ppmv}$ ,  $41.4\text{ ppmv}$ , and  $23.9\text{ ppmv}$  for QTF1, QTF2, and QTF1+QTF2, respectively, was obtained. The M-QEPAS resulted in a significantly improved MDL. The corresponding calculated normalized noise equivalent absorption coefficients (NNEA) were  $11.55\text{ cm}^{-1}\text{W}/\sqrt{\text{Hz}}$ ,  $10.31\text{ cm}^{-1}\text{W}/\sqrt{\text{Hz}}$ , and  $5.95 \times 10^{-8}\text{ cm}^{-1}\text{W}/\sqrt{\text{Hz}}$ , respectively.

In conclusion, we demonstrated a trace gas detection scheme of M-QEPAS in which two QTFs were used as

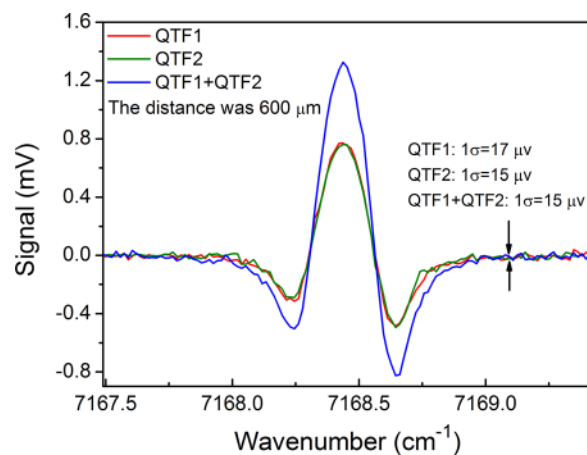


FIG. 5. Measured signal and noise at modulation depth of  $0.492\text{ cm}^{-1}$ .

acoustic transducer. Compared with QEPAS sensor using single QTF, M-QEPAS employing two QTFs had a signal enhancement of 1.7 times for the same operating conditions. A smaller difference in resonant frequency and phase of QTFs will result in greater signal improvement. Furthermore, the detection sensitivity of M-QEPAS can be further improved by using more than two QTFs and with the use of acoustic micro-resonator tubes.

This work was supported by the Special Financial Grant from the China Postdoctoral Science Foundation (No. 2015T80350), the Natural Science Foundation of Heilongjiang Province of China (Grant No. F2015011), a postdoctoral fund of Heilongjiang Province (Grant No. LBH-Z14074), the Fundamental Research Funds for Central Universities (Grant No. HIT. NSRIF. 2015044), the General Financial Grant from the China Postdoctoral Science Foundation (Grant Nos. 2014M560262 and 2013M531040), and the National Key Scientific Instrument and Equipment Development Projects of China (No. 2012YQ040164).

- <sup>1</sup>T. Mitsui, M. Miyamura, A. Matsunami, K. Kitagawa, and N. Arai, *Clin. Chem.* **43**, 1993 (1997).
- <sup>2</sup>W. Ren, A. Farooq, D. F. Davidson, and R. K. Hanson, *Appl. Phys. B* **107**, 849 (2012).
- <sup>3</sup>A. Elia, P. M. Lugarà, C. di Franco, and V. Spagnolo, *Sensors* **9**, 9616 (2009).
- <sup>4</sup>A. A. Kosterev, Y. A. Bakhirkin, R. F. Curl, and F. K. Tittel, *Opt. Lett.* **27**, 1902 (2002).
- <sup>5</sup>Y. F. Ma, R. Lewicki, M. Razeghi, and F. K. Tittel, *Opt. Express* **21**, 1008 (2013).
- <sup>6</sup>L. Dong, V. Spagnolo, R. Lewicki, and F. K. Tittel, *Opt. Express* **19**(24), 24037 (2011).
- <sup>7</sup>K. Liu, X. Y. Guo, H. M. Yi, W. D. Chen, W. J. Zhang, and X. M. Gao, *Opt. Lett.* **34**, 1594 (2009).
- <sup>8</sup>S. Borri, P. Patimisco, I. Galli, D. Mazzotti, G. Giusfredi, N. Akikusa, M. Yamanishi, G. Scamarcio, P. De Natale, and V. Spagnolo, *Appl. Phys. Lett.* **104**, 091114 (2014).
- <sup>9</sup>Y. C. Cao, W. Jin, L. H. Ho, and Z. B. Liu, *Opt. Lett.* **37**, 214 (2012).